Opt Quant Electron (2016) 48:467
DOI 10.1007/s11082-016-0742-4

CrossMark

The effects of DC power on the physical properties and surface topography of sputtered TiN nanostructured thin films

Nader Ghobadi[1] · Mohsen Ganji[1] · Carlos Luna[2] · Azin Ahmadpourian[3] · Ali Arman[4]

Received: 9 August 2016 / Accepted: 13 September 2016 / Published online: 21 September 2016
© Springer Science+Business Media New York 2016

Abstract Four high quality nanostructured thin films of titanium nitride, with thicknesses equal to 81, 325, 485 and 565 nm respectively, were deposited on glass substrates by the reactive magnetron sputtering method using different DC power values (from 200 to 410 W). The results revealed that the DC power plays a crucial role in the evolution of the thickness, topography, microstructure, optical and semiconducting properties of the resulting thin films. Specifically, an increase in the DC power enhances the crystalline order of the samples, consequently; the energy band gap values and the electrical resistivity decrease. Also, a competitive growth of crystalline planes of different orientations was found as a consequence of the increment of the grain size. In addition, the influence of DC power on the 3-D surface morphology of these thin films was investigated. The largest peak height and also the largest valley depth from the mean surface increased at higher amounts of DC power. The flexible variation of the physical properties of thin films with the simple and reproducible variation of the DC power in the sputtering process could be exploited in the use of these samples in specific technological applications.

Keywords Nanostructured thin films · Magnetron sputtering · DC power · TiN · Surface topography

✉ Nader Ghobadi
n.ghobadi@malayeru.ac.ir

[1] Physics Department, Faculty of Science, Malayer University, Malayer, Iran

[2] Facultad de Ciencias Físico Matemáticas, Universidad Autónoma de Nuevo León, Av. Pedro de Alba s/n, 66455 San Nicolás de los Garza, Nuevo León, Mexico

[3] Departments of Physics, Kermanshah Branch, Islamic Azad University, Kermanshah, Iran

[4] Young Researchers and Elite Club, Kermanshah Branch, Islamic Azad University, Kermanshah, Iran

1 Introduction

Because of their suitable mechanical properties, high hardness and noticeable chemical and thermal stability, titanium nitride (TiN) thin films are widely used in various industries as protective and abrasion-resistant coatings (Ma et al. 2006), being materials relatively harder than their bulk analogous due to their reduced size and interfacial effects (Ma et al. 2007; Patsalas et al. 2000). On the other hand, the electrical resistivity and the semiconductor properties of TiN thin films are usually considerably influenced by their grain size and surface morphology, which in turn are strongly affected by the synthetic conditions employed in their deposition. For instance, depositing TiN coatings at sufficiently high temperatures leads to layers of densities close to that of the stoichiometric bulk matter (Petrov 2003). Moreover, increasing the content ratio of nitrogen to argon in the plasma atmosphere results in the decrement of the deposition rate and grain size of these films (Popović et al. 2004). In addition, researchers have found that the film surface roughness is proportional to the grain size (Pelleg et al. 1991), and that increasing the kinetic energy of plasma ions raises the intensity of XRD peaks, increases the grain size and changes the crystallographic orientation of the deposited layers (Köstenbauer et al. 2007). In this regard, it has been reported that TiN films with thickness of few tens of nanometers exhibit (200)-orientation, whereas TiN layers with thicknesses of few hundreds of nm are (111)-oriented films (Hultman 2000). The correlation between these changes in the microstructural properties with the synthetic conditions, and with the 3-D surface morphology and physical properties of TiN thin films is a current research topic with important technological implications.

In the present work, the role of the DC power on the growth and physical properties of nanostructured TiN thin films deposited by reactive magnetron sputtering method have been investigated in detail.

2 Experimental procedures

The sputtering system used to prepare the samples has been described elsewhere (Gelali et al. 2012; Molamohammadi et al. 2015; Ghodselahi and Arman 2015; Arman et al. 2015a). A titanium disk of very high purity (more than 99 %) and four glass substrates were used in the deposition process. The substrates were washed in trichloroethylene, acetone, alcohol and distilled water respectively, using an ultrasonic system. Afterwards, the residual surface contamination was removed by ion bombardment in pure argon plasma for ten minutes. The target (titanium disk) was set on a plane magnetron in the vacuum chamber, and the target holder had a negative bias (i.e. the target was on the cathode), whereas the vacuum chamber and substrates holders were in the anode of the system. Then, a very thin titanium layer was deposited on substrates using only Ar for 10 min, which is suitable for increasing the adhesion of the main film and to reduce the residual stress between the TiN film and the substrate (Sundgren 1985).

In this study four TiN thin films (named S-1, S-2, S-3 and S-4, respectively) were deposited on glass substrates at different amounts of DC power (from 200 to 410 W). Other experimental parameters were fixed as follows: Ar flow rate: 40 sccm (standard cubic centimeters per minute), N_2 flow rate: 2 sccm, base pressure: 3×10^{-5} mbar, working pressure: 2.4×10^{-3} mbar, deposition time: 2 h, substrate temperature: 400 °C.

The crystalline phases present in samples and their crystalline orientation were investigated using an X-ray diffraction system (XRD) with Cu Kα (λ = 1.54060 Å) radiation. The average crystal sizes were calculated from the data of the more intense diffraction peaks with the Scherrer equation (Chawla et al. 2008):

$$L_{(hkl)} = \frac{0.9\lambda}{\beta \cos\theta} \tag{1}$$

where λ is the X-ray wavelength, β is the broadening of the diffraction peak (after subtracting the instrumental broadening), and θ is the diffraction angle at which the peak maximum occurs.

The surface topography of the four samples was investigated by an AFM system in non-contact mode using a Nanoscope Multimode atomic force microscope (Digital Instruments, Santa Barbara, CA) and scan rates of 10–20 μm/s to obtain images over square areas of 4.4 μm × 4.4 μm. The measurements were performed at room temperature using cantilevers with the nominal properties for force-distance curve measurements. In order to describe the morphology of samples, the power spectral density (PSD) function of the bidirectional reflectance distribution function (BRDF) was analyzed from the AFM data (Kulesza and Bramowicz 2014; Arman et al. 2015b).

The ultraviolet–visible spectra of the nanostructured thin films were recorded using a UV–Vis spectrometry (Perkin-Elmer, UV/VIS Spectrometer Lambda25-USA) in a

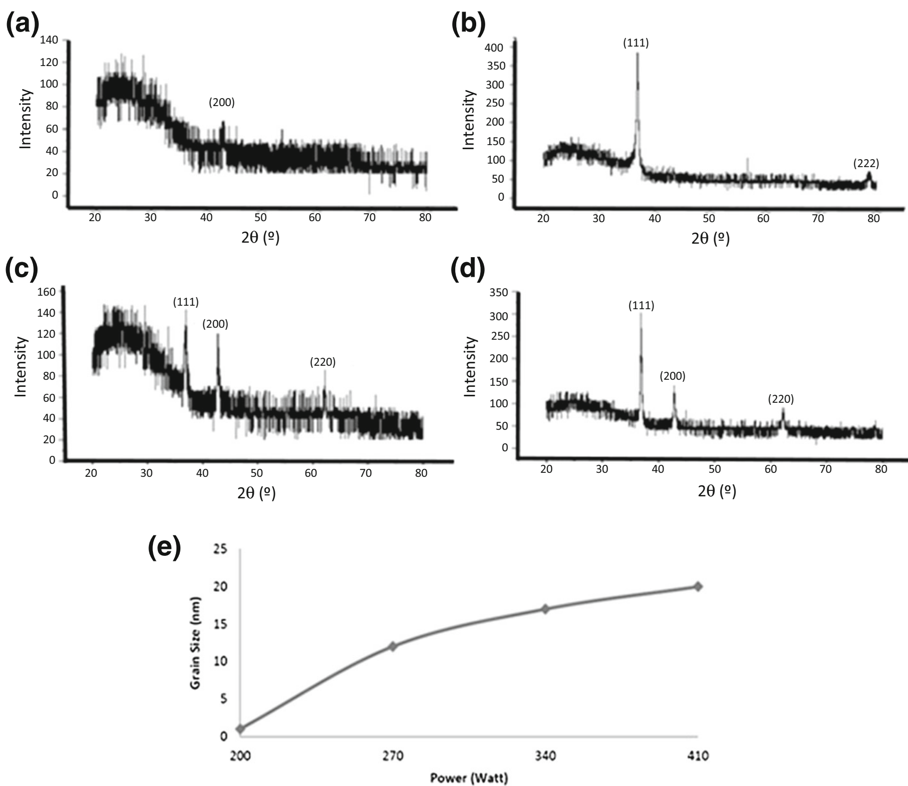

Fig. 1 XRD patterns of samples: **a** S-1, **b** S-2, **c** S-3, **d** S-4 and **e** grain size of the prepared layers versus the DC power

wavelength range of 190–1100 nm. To determine the direct band gap of the four thin films, plots of $(Ah\nu)^2$ versus hν were analyzed using a revisited Tauc's method (the ineffective thickness model), introduced elsewhere (Ghobadi et al. 2016).

3 Results and discussion

The XRD patterns of the four samples are shown in Fig. 1. It is observed that the crystalline order degree of the film S-1 (Fig. 1a) is relatively low in comparison with the other three films, showing only a very weak diffraction peak associated to the (200) crystallographic planes of the cubic TiN structure (JCPDS 38-1420). However, sample S-2 exhibits

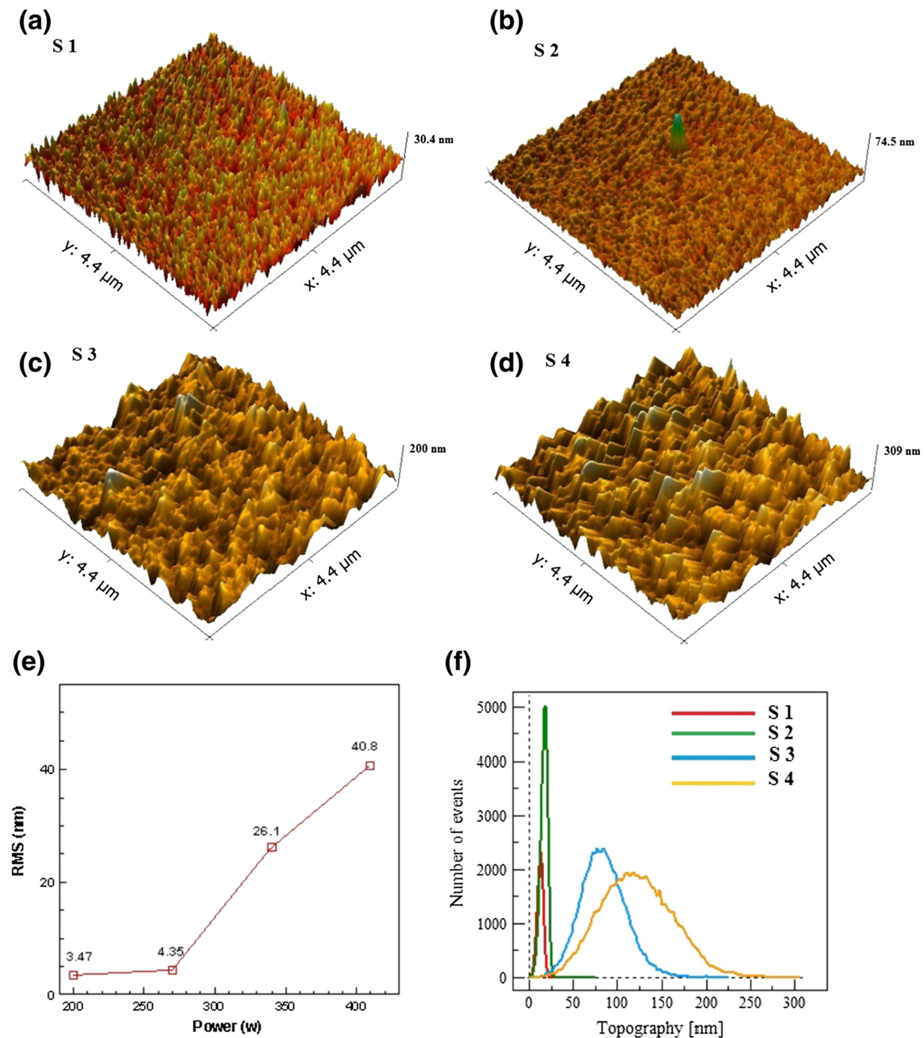

Fig. 2 Representative AFM images of samples: **a** S-1, **b** S-2, **c** S-3, **d** S-4, **e** surface roughness as a function of the DC power and **f** particle size distribution curves of the four samples

an intense and well-defined (111) diffraction peak and a weak (222) peak (Fig. 1b), indicating that an applied DC power of 270 W favors the growth of (111) orientated grains. Increasing the kinetic energy of Ar^+ ions using a DC power of 340 W (sample S-3), leads to the formation of additional (200) and (220) planes (Fig. 1c), and the relative intensity of these peaks decreased in comparison with that of the (111) peak for sample S-4, which was obtained using a DC power of 410 W (Fig. 1d). The average crystal size of the samples was estimated using the Scherrer equation and it has been plotted as a function of the amount of power supply used in the preparation of samples (Fig. 1e). The ascending behavior of this curve confirms the increase in crystal order of the films due to the increase of the kinetic energy of the plasma ions.

Representative 3D-AFM images are presented in Fig. 2a–d. Surface roughness (RMS) as a function of DC power, and the size distribution of heights obtained from the AFM images are shown in Fig. 2e, f, respectively. It can be seen that samples S-1 and S-4 have the lowest and highest values of surface roughness, respectively. Also, it is observed that the RMS values are correlated with the particle size distribution curves: Gaussian curve corresponding to sample S-1 has the smallest width; therefore this sample has more equal-height points as well as a smoother surface than the other samples. On the other hand, the Gaussian curve corresponding to sample S-4 has the largest width and the less equal-height points; consequently this sample has a rougher surface in comparison with those of the other samples.

Table 1 shows the characteristic parameters that describe the surface characterization of the AFM images (according with ISO 25178-2: 2012) (http://www.digitalsurf.fr; http://www.iso.org): root-mean-square deviation (S_q), skewness (S_{sk}) and kurtosis (S_{ku}) of topography height distribution, the largest peak height value (S_p) and the largest valley depth (S_v) value from the mean/reference surface within the sampling area, the sum of the largest peak height value and largest valley depth value within the sampling area ($S_z = S_p + S_v$), and the arithmetical mean height that is the mean surface roughness (S_a).

Table 1 Preparation conditions and some properties of the studied thin films

	S-1	S-2	S-3	S-4
Preparation parameters of the four samples				
Power (W)	200	270	340	410
Voltage (V)	255	310	365	430
Current (A)	0.78	0.87	0.93	0.95
Deposition rate (nm/min)	0.68	2.7	4	4.72
Samplés properties				
Thickness (nm)	81	325	485	565
Energy band gap (eV)	3.81	3.57	3.35	3.35
Electrical resistivity (μΩ cm)	900	500	180	160
Rms (S_q) (nm)	3.47	4.35	26.1	40.8
S_{sk}	−0.144	0.998	0.423	0.265
S_{ku}	2.95	16	3.85	30.01
S_p (nm)	17.3	56.9	142	185
S_v (nm)	13.1	17.6	85.2	123
S_z (nm)	30.4	74.5	227	309
S_a (nm)	2.78	3.25	20.4	32.8

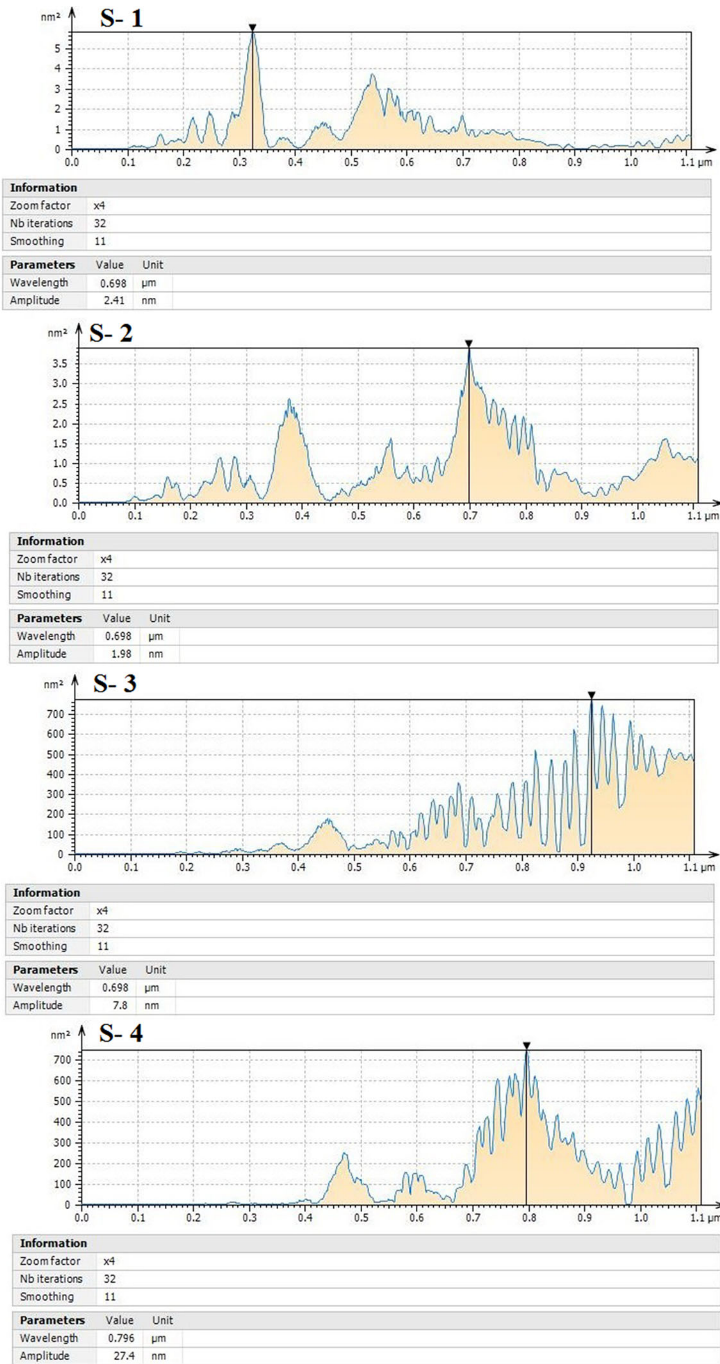

Fig. 3 The averaged power spectral density (surface) of the four samples calculated for scanning square areas of 4.4 µm × 4.4 µm

It is observed that most of these parameters tend to increase as the DC power increases, in correlation with the variations of the mean particle size. However, the skewness displays fluctuating values.

The PSD function of the four samples was studied using Fast Fourier Transforms (FFT). According to Fig. 3 the wavelength of the samples were found at 0.700 μm and the following amplitudes: (S1) 0.730 nm, (S2) 0.833 nm, (S3) 7.01 nm and (S4) 11.6 nm.

The UV–Vis spectra of the samples are shown in Fig. 4a. Such spectra revealed a blue shift with decreasing DC power. Based on the fact that a smaller nanoparticle size will

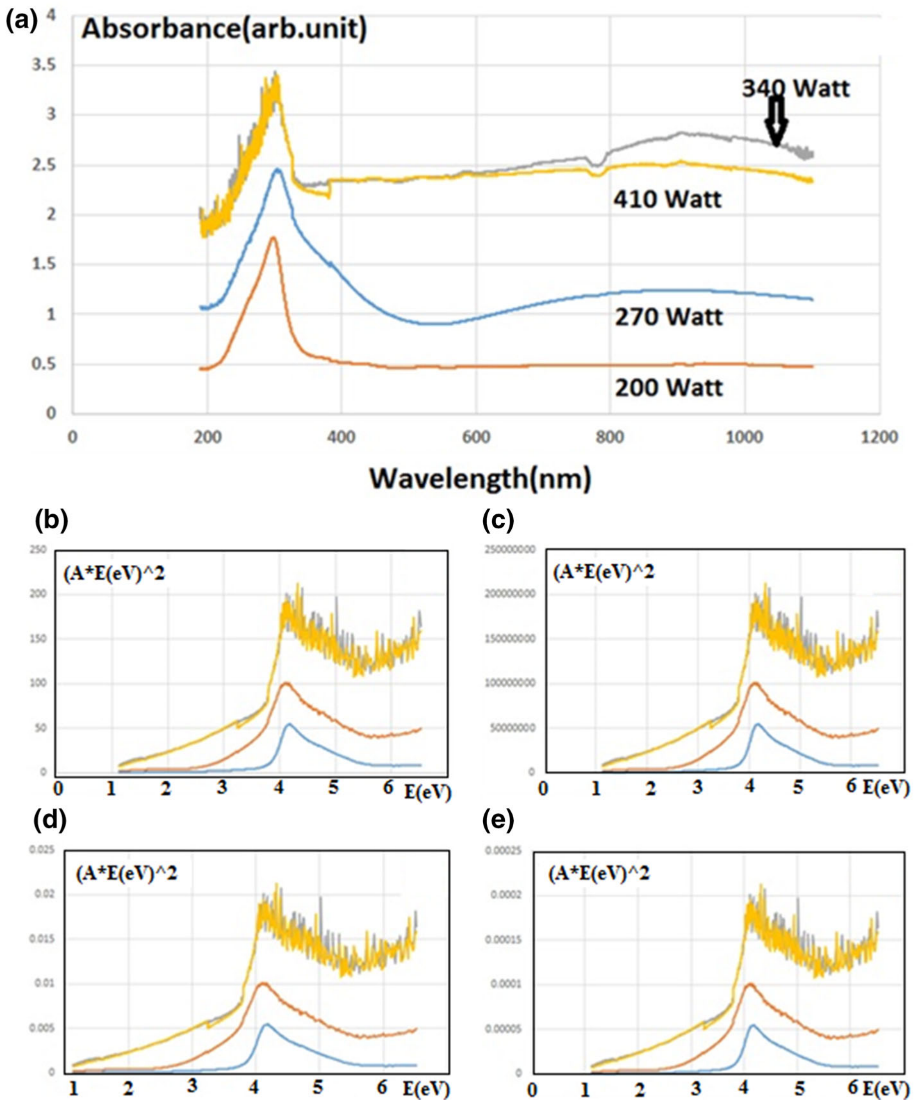

Fig. 4 **a** UV–visible spectra of the four samples with different DC powers. Plot of $(Ah\nu)^2$ versus $(h\nu)$ for samples with different DC powers and considering different thickness values: **b** thickness = t_0, **c** thickness = 1000 t_0, **d** thickness = 0.01 t_0 and **e** thickness = 0.001 t_0

result in an absorption edge at smaller wavelengths, the observed blue shift should be due to a decrease in nanoparticles size (Molamohammadi et al. 2015). In addition, the band-gap energy calculated from these spectra (Table 1) decreases from 3.81 to 3.32 eV as the DC power increases from 200 to 410 W.

The lack of dependence of the revisited Tauc's method on the film thickness has been shown, in Fig. 4b–e, by varying the films' thicknesses by six orders of magnitude. It's been shown that "an absorbance data for each sample has a unique optical band gap" and a supposed different thickness doesn't change the optical band gap. Therefore, researchers can determine the optical band gap of the thin films without thickness measurement, because they are required by this method to have in hand the absorbance spectra and not the absorption coefficient (Ghobadi 2015).

Moreover, the electrical resistivity of the deposited films was studied (Table 1) observing that it decreases as the sputtering DC power increases, which is in agreement with the increment of the grain size.

4 Conclusions

The effects of DC power changes (from 200 to 410 W) on the microstructure, 3-D surface morphology and the optical, electrical and semiconductor properties of TiN thin films, prepared by reactive DC magnetron sputtering, have been analyzed. XRD patterns revealed a complex competition of crystalline planes growth as the average particle size is increased through the increase of the DC power used during the deposition process. AFM images showed that the average grain size, the root-mean-square deviation and other topography parameters tend to increase as the DC power is increased. In addition, the optical band-gap energy decreases from 3.81 to 3.32 eV, and the electrical resistivity decreases from 900 to 160 μΩ cm. The dependencies reported in the present work can be exploited in the modulation of the physical properties of thin TiN films for specific applications.

References

Arman, A., Ghodselahi, T., Molamohammadi, M., Solaymani, S., Zahrabi, H., Ahmadpourian, A.: Microstructure and optical properties of Cu@ Ni nanoparticles embedded in aC: H. Prot. Met. Phys. Chem. Surf. **51**(4), 575–578 (2015a)

Arman, A., Ţălu, Ş., Luna, C., Ahmadpourian, A., Naseri, M., Molamohammadi, M.: Micromorphology characterization of copper thin films by AFM and fractal analysis. J. Mater. Sci.: Mater. Electron. **26**(12), 9630–9639 (2015b)

Chawla, V., Jayaganthan, R., Chandra, R.: Structural characterization of magnetron sputtered nanocrystalline TiN thin films. Mater. Charact. **59**, 1015–1020 (2008)

Gelali, A., Ahmadpourian, A., Bavadi, R., Hantehzadeh, M.R., Ahmadpourian, A.: Characterization of microroughness parameters in titanium nitride thin films grown by DC magnetron sputtering. J. Fusion Energy **31**(6), 586–590 (2012)

Ghobadi, N.: Derivation of ineffective thickness method for investigation of the exact behavior of the optical transitions in nanostructuredthin films. J. Mater. Sci.: Mater. Electron. (2015). doi:10.1007/s10854-016-4925-3

Ghobadi, N., Ganji, M., Luna, C., Arman, A., Ahmadpourian, A.: Effects of substrate temperature on the properties of sputtered TiN thin films. J. Mater. Sci.: Mater. Electron. **27**, 2800–2808 (2016)

Ghodselahi, T., Arman, A.: Magnetoresistance of Cu–Ni nanoparticles in hydrogenated amorphous carbon thin films. J. Mater. Sci.: Mater. Electron. **26**(6), 4193–4197 (2015)

Hultman, L.: Thermal stability of nitride thin films. Vacuum **57**, 1–30 (2000)

ISO 25178-2: 2012, Geometrical product specifications (GPS)—Surface texture: Areal—Part 2: Terms, definitions and surface texture parameters. http://www.iso.org. Accessed 28 Mar 2015

Köstenbauer, H., Fontalvo, G.A., Kapp, M., Keckes, J., Mitterer, C.: Annealing of intrinsic stresses in sputtered TiN films: the role of thickness-dependent gradients of point defect density. Surf. Coat. Technol. **201**, 4777–4780 (2007)

Kulesza, S., Bramowicz, M.: A comparative study of correlation methods for determination of fractal parameters in surface characterization. Appl. Surf. Sci. **293**, 196–201 (2014)

Ma, C.H., Huang, J.H., Chen, H.: Nanohardness of nanocrystalline TiN thin films. Surf. Coat. Technol. **200**, 3868–3875 (2006)

Ma, L.W., Cairney, J.M., McGrouther, D., Hoffman, M., Munroe, P.R.: Three dimensional imagine of deformation modes in TiN based thin films coatings. Thin Solid Films **515**, 3190–3195 (2007)

Molamohammadi, M., Luna, C., Arman, A., Solaymani, S., Boochani, A., Ahmadpourian, A., Shafiekhani, A.: Preparation and magnetoresistance behavior of nickel nanoparticles embedded in hydrogenated carbon film. J. Mater. Sci.: Mater. Electron. **26**(9), 6814–6818 (2015a)

Molamohammadi, M., Arman, A., AchourB, A., Astinchap, A., Ahmadpourian, A., Boochani, S., Naderi, A.Ahmadpourian: Microstructure and optical properties of cobalt–carbon nanocomposites prepared by RF-sputtering. J. Mater. Sci.: Mater. Electron. **26**(8), 5964–5969 (2015b)

Mountains Map® 7 Software (Digital Surf, Besançon, France). http://www.digitalsurf.fr. Accessed 28 Mar 2015

Patsalas, P., Charitidis, C., Logothetidis, S.: The effect of substrate temperature and biasing on the mechanical properties and structure of sputtered titanium nitride thin films. Surf. Coat. Technol. **125**, 335–340 (2000)

Pelleg, J., Zevin, L.Z., Lungo, S.: Reactive-sputter-deposited TiN films on glass substrates. Thin Solid Films **197**, 117–128 (1991)

Petrov, I.: Microstructural evolution during film growth. J. Vac. Sci. Technol. **21**, S117–S128 (2003)

Popović, N., Bogdanov, Ž., Goncić, B., Zec, S., Rakočević, Z., Zlatanović, M., Peruško, D.: TiN thin films deposited by ion beam sputtering: effects of energetic particles bombardment. Thin Solid Films **459**, 286–291 (2004)

Sundgren, J.E.: Structure and properties of TiN coatings. Thin Solid Films **128**, 21–44 (1985)